3.3 Strongly Correlated Quantum Systems

Theoretical study of strongly correlated topological phenomena and its application to machine learning

Yukitoshi MOTOME

Department of Applied Physics,

The University of Tokyo, Bunkyo, Tokyo 113-8656

We have theoretically studied a variety of intriguing topological phenomena in strongly-correlated electron systems by using numerical methods including first-principles calculations, quantum many-body calculations, and machine learning (project numbers: 2023-Ca-0066 and 2023-Cb-0014). During the last fiscal year, we have achieved substantial progress on the following topics.

(i) *Development of new theoretical methods and their applications*: We proposed a new scheme for physical reservoir computing by using interacting spin systems as reservoirs [1]. In addition, inversely exploiting the framework of quantum reservoir computing, we developed a new theoretical tool to investigate the nature of quantum systems, called "quantum reservoir probing", and applied it to quantum scrambling [2] and quantum phase transitions [3]. We also applied the inverse Hamiltonian design that we developed to discover new Hamiltonians with maximized quantum entanglement [4].

(ii) *Kitaev quantum spin liquids and its realization in experiments*: We unveiled how the Kitaev spin liquid meets spin nematics in the S=1 Kitaev model with bilinear-biquadratic interactions by using the SU(3) formalism [5]. We also clarified the origin of a chiral spin liquid found in the competing region [6]. In addition, by using the pseudo-fermion functional renormalization group method, we clarified the ground-state phase diagram of the Kitaev-Heisenberg model on a three-dimensional hyperhoneycomb lattice [7]. We also revealed that the Kitaev spin liquid exhibits a peculiar inter-edge resonance [8] and spin Seebeck effect [9]. We also studied effects of dissipation in the non-Hermitian Kitaev model under a magnetic field [10]. Furthermore, we proposed new experimental platforms in heterostructures composed of van der Waals magnets [11] and ilmenite oxides [12], and rare-earth magnets [13].

(iii) *Topological properties of Weyl semimetals*: By using first-principles calculations, we unveiled magnetic, transport, and topological properties of atomically thin films of Co-based shandite [14]. We also extend the study to topological transitions in the kagome monolayer by rotating the magnetic field [15].

(iv) *Topological spin crystals as spin moire*: Extending the research until the last years, we

clarified the behavior of emergent electric fields arising from magnetic resonance in a one-dimensional chiral magnet [16]. In addition, we revealed an instability of magnetic skyrmion strings by a spin current [17]. We also wrote an article on spin moire in 日本物理学会誌 [18].

(v) *Collaborations with experimental groups*: We made fruitful collaborations on experiments for amorphous Fe-Sn thin films [19], high-field phase diagram of a chiral antiferromagnet showing quadrupole ordering [20], orbital-selective band reconstruction in $TaTe_2$ [21], the evolution of Floquet bands under circularly polarized light [22], and the noncoplanar antiferromagnetic structures in $DyTe_3$ [23].

References

[1] K. Kobayashi and Y. Motome, Sci. Rep. **13**, 15123 (2023).

[2] K. Kobayashi and Y. Motome, preprint (arXiv:2308.00898).

[3] K. Kobayashi and Y. Motome, preprint (arXiv:2402.07097).

[4] K. Inui and Y. Motome, preprint (arXiv:2402.15802).

[5] R. Pohle, N. Shannon, and Y. Motome, Phys. Rev. B **107**, L140403 (2023).

[6] R. Pohle, N. Shannon, and Y. Motome, preprint (arXiv:2404.11623).

[7] K. Fukui, Y. Kato, and Y. Motome, J. Phys. Soc. Jpn. **92**, 064708 (2023).

[8] T. Misawa, J. Nasu, and Y. Motome, Phys. Rev. B **108**, 115117 (2023).

[9] Y. Kato, J. Nasu, M. Sato, T. Okubo, T. Misawa, and Y. Motome, preprint (arXiv:2401.13175).

[10] K. Fukui, Y. Kato, and Y. Motome, preprint (arXiv:2402.05516).

[11] L. Zhang and Y. Motome, preprint (arXiv:2310.01075).

[12] Y.-F. Zhao, S.-H. Jang, and Y. Motome, preprint (arXiv:2403.09112).

[13] S.-H. Jang and Y. Motome, preprint (arXiv:2402.18837).

[14] K. Nakazawa, Y. Kato, and Y. Motome, Commun. Phys. **7**, 48 (2024).

[15] K. Nakazawa, Y. Kato, and Y. Motome, preprint (arXiv:2402.16273).

[16] K. Shimizu, S. Okumura, Y. Kato, and Y. Motome, Phys. Rev. B **108**, 134436 (2023).

[17] S. Okumura, V. P. Kravchuk, and M. Garst, Phys. Rev. Lett. **131**, 066702 (2023) [selected as Editor's suggestion].

[18] 清水宏太郎、奥村駿、加藤康之、求 幸年: 日本物理学会誌 **78**, 314 (2023).

[19] K. Fujiwara *et al.*, Nat. Commun. **14**, 3399 (2023).

[20] T. Nomura *et al.*, Phys. Rev. B **108**, 054434 (2023).

[21] N. Mitsuishi *et al.*, Phys. Rev. Research **6**, 013155 (2024).

[22] Y. Hirai *et al.*, Phys. Rev. Research **6**, L012027 (2024).

[23] S. Akatsuka *et al.*, Nat. Commun., in press.

Analysis of *ab initio* Hamiltonians for molecular solid $(TMTTF)_2PF_6$ under pressure

Takahiro Misawa
Institute for Solid State Physics, University of Tokyo
Kashiwa-no-ha, Kashiwa, Chiba 277-8581

Organic conductors are widely studied due to the diverse physical properties that arise from the interactions of charge, spin, and lattice degrees of freedom. These interactions lead to various electronic states, including superconductivity, magnetic ordering, and charge ordering. In fact, crystals made of TMTTF molecules exhibit all these electronic states when external pressure is applied and have been the subject of active research for over 40 years. By combining these findings with results from related compounds made of TMTSF molecules, a unified pressure-temperature phase diagram has been discussed. However, there has not yet been a quantitative analysis of how external pressure impacts electron correlations in these systems, nor an understanding of what factors control the various phases under pressure.

In this project, we have performed a combined experimental and theoretical analysis of the pressure-dependent physical properties of the quasi-one-dimensional organic conductor $(TMTTF)_2PF_6$ [1]. We obtain the crystal structures under pressure by performing x-ray diffraction measurements for single crystals of $(TMTTF)_2PF_6$ with a diamond anvil cell up to 8 GPa. Based on the obtained crystal structures, we first derive the low-energy effective Hamiltonians for $(TMTTF)_2PF_6$ under pressure using Quantum ESPRESSO [2] and RESPACK [3]. We obtained the following characteristic features of the microscopic parameters in the low-energy effective Hamiltonians: (1) By applying the pressure, the transfer integrals increase, whereas the screened Coulomb interactions decrease, resulting in a drastic reduction of correlation effects. For example, the normalized onsite Coulomb interaction ($U/\bar{t}_a$) decreases from 12 at ambient pressure to 6 at 8 GPa. (2) The degree of dimerization in the intrachain transfer integrals, as the result of the decrease in structural dimerization together with the change in the intermolecular configuration, almost disappears above 4 GPa.

Then, we solve the low-energy effective Hamiltonians by using the many-variable variational Monte Carlo method [4, 5], which effectively treats electron correlation effects. We find that the charge ordering is substantially suppressed above 1 GPa while the spin ordering survives up to higher pressure. This theoretical result is consistent with the temperature dependence of the resistivity under pressure.

Changes in the electronic states of molecular solids under pressure have been studied as a typical example of pressure effects on strongly correlated electron systems. The present study demonstrates that recent advances in high-pressure experimental and computational tech-

niques now enable a quantitative microscopic analysis of physical properties under pressure.

References

[1] M. Itoi, K. Yoshimi, H. Ma, T. Misawa, *et al.*, arXiv:2403.13816.

[2] P. Giannozzi *et al.*, J.of Phys.: Cond. Matt. **29**, 465901 (2017).

[3] K. Nakaramu *et al.*, Comp. Phys. Comm. **261**, 107781 (2021).

[4] T. Misawa *et al.*, Comp. Phys. Comm. **235**, 447 (2019).

[5] https://www.pasums.issp.u-tokyo.ac.jp/mvmc/en/

On the relation between artificial neural networks and tensor networks

Yusuke NOMURA

Institute for Materials Research (IMR), Tohoku University,

2-1-1 Katahira, Aoba-ku, Sendai 980-8577, Japan

Accurate representation of quantum states is a grand challenge in computational physics. Recently, a new method based on artificial neural networks has been introduced. This is an attempt to describe the quantum many wave functions using artificial neural networks and approximate quantum states with high precision using a much smaller number of parameters than the actual dimension of the wave function.

This artificial neural network method is complementary to tensor network methods [1]. Both artificial neural networks and tensor networks have the property of universal approximation in the limit of infinite hidden degrees of freedom and bond dimensions, respectively. However, they are currently being developed independently.

In this project, we try to develop a more compact and efficient quantum state representation formalism by exploring a new network formalism that combines artificial neural networks and tensor networks. As a first step, in this fiscal year, we have tried to investigate the relation between the two types of networks.

In more detail, we performed a supervised learning to learn the relation between spin configurations σ and amplitude of wave function $\psi(\sigma)$ for one-dimensional quantum spin systems. The training data was generated using a small system size that allows for exact diagonalization [set of σ and $\psi(\sigma)$]. Then, we compare the representative ability between restricted Boltzmann machines (RBM) and matrix product states (MPS) by performing supervised learning of quantum states. It is well known that MPS is a very efficient ansatz for representing quantum states for one-dimensional systems. Surprisingly and interestingly, the performance of RBM is comparable to MPS when the number of parameters is the same between the two architectures.

This indicates that artificial neural networks have an excellent ability to represent quantum states. In the future, we will investigate the possibility of combining artificial neural networks with tensor networks to better represent quantum states.

References

[1] Y. Nomura, J. Phys.: Condens. Matter **36** 073001 (2024)

Long-time simulation for strongly-correlated quantum systems

Masatoshi IMADA
Research Institute for Sicence and Engineering, Waseda University,
3-4-1 Okubo, Shinjuku-ku, Tokyo, 169-8555
Department of Engineering and Applied Sciences, Sophia University.
7-1 Kioi-cho, Chiyoda-ku Tokyo, 102-8554

In this report, we review recent progress in development of the algorithm and its benchmark examined for forecast of the long-time behavior of the quantum many-body dynamics by utilizing short-time reliable quantum-dynamics data [1]. For the purpose of this challenging long-time forecast, here, the dynamic mode decomposition (DMD) employed in the field of fluid dynamics [2,3] has been employed. The DMD is advantageous in its simplicity and versatility. The dominant part of the computational cost is primarily scaled by that of singular value decomposition (SVD) of a certain matrix constructed from the short-time data.

This method has enabled accurate predictions of the quantum many-body dynamics at nearly one order of magnitude longer time than the range of utilized short-time training data even when the long-time behavior exhibits complex features such as multiple oscillations and power-law decay to a nonzero constant. The benchmark was performed by taking the transverse-field Ising models as model systems.

For more realistic situations, the method has applied to noisy input data as well. The DMD prediction has turned out to be still accurate when the noise level is within a few percent of the noiseless part. Furthermore, systematic and statistical errors of the DMD prediction have also been estimated in this work, which shows essentially slow growth of the estimated error ensuring the reliability of the forecast at nearly one order longer time than the time of input training data.

The findings indicate that the DMD is equally a promising tool for the dynamics of other quantum many-body systems that are difficult to simulate by conventional direct numerical simulations by the time evolution of the many-body wave functions. The DMD is powerful and versatile even at quantum critical points with temporary long-ranged quantum fluctuations characteristic of the growing quantum entanglement. Because of the versatile nature of the algorithm, the method is also expected to be applicable to the time series of experimental data in quantum many-body systems, which is left for future studies.

This review of the activity is based on the results achieved by Ryui Kaneko collaborated with Yoshiyuki Kabashima, Tomi Ohtsuki and the author. The project was financially supported by MEXT KAKENHI, Grant-in-Aid for Transformative Research Area (Grant No. JP22H05111 and No. JP22H05114). and also supported by MEXT under the grant number JPMXP1020230411.

References

[1] R. Kaneko, M. Imada, Y. Kabashima and T. Ohtsuki: arXiv:2403.19947.

[2] C. W. Rowley, I. Mezić, S. Bagheri, P. Schlatter, and D. S. Henningson, J. Fluid Mech. **641**, 115 (2009).

[3] P. J. Schmid: J. Fluid Mech. **656**, 5 (2010).

Development of Variational-Wave-Function Spectroscopy for Quantum Materials

Youhei YAMAJI
Research Center for Materials Nanoarchitectonics, National Institute for Materials Science
Namiki, Tsukuba-shi, Ibaraki 305-0044

It is known that direct observation of quantum entanglement in many-body systems is difficult. Currently, detailed analysis on signatures of the entanglement in spectroscopy measurements has been conducted on one-dimensional quantum spin chains, which are the simplest yet exhibit macroscopic quantum entanglement [1]. Thus, it is desirable to explore numerical spectroscopy flexibly applicable to complicated quantum materials.

Variational wave function methods provide a promising foundation for numerical spectroscopy. However, there had been a difficulty: As discussed in the literature [2], it is difficult to find a concise representation of the summation of two variational wave function. Once we design a variational wave function, we can define a subspace of the many-body Hilbert space, $\mathcal{J}$. However, it is not easy to find $|\psi_3\rangle \in \mathcal{J}$ that satisfies $|\psi_3\rangle = c_1|\psi_1\rangle + c_2|\psi_2\rangle$ $(c_1, c_2 \in \mathbb{C})$ for $|\psi_1\rangle,\ |\psi_2\rangle \in \mathcal{J}$. For example, it is formidable for the subspace $\mathcal{J}$ spanned by variational wave functions implemented in an open source software, mVMC [3].

A simple solution is, instead of taking summation, taking inner products, such as $\langle\psi_1|\psi_2\rangle$, and expectation values, $\langle\psi_1|\hat{O}|\psi_2\rangle$, of a given operator $\hat{O}$ among the bases. While it is again not easy because of large statistical noise in sampling for $\langle\psi_1|\psi_2\rangle$, an efficient sampling has been proposed [4] and implemented [5].

To simulate whole inelastic neutron scattering spectra, the order of $N_{\rm s}^2$ bases, where $N_{\rm s}$ is the number of electrons, are required. Angle resolved photoemission spectroscopy simulation requires more bases.

Then, the bottleneck of the method is the memory and computational costs for the generalized eigenvalue problems defined by the nonorthogonal basis set. During the maintenance of reasonable statistics to estimate the inner products, which favor the flat MPI model, we need to utilize relatively small memory per process. In the present study, to reduce memory costs and to reach $N_{\rm s} > 100$, we implemented the LOBCG [6] method and a block-type variation of the Sakurai-Sugiura method [7].

References

[1] For example, P. Laurell, *et al.*: Phys. Rev. Lett. **127**, 037201 (2021).

[2] For example, W.-L. Tu, *et al.*: Phys. Rev. B **103**, 205155 (2021).

[3] T. Misawa, *et al.*: Comput. Phys. Commun. **235**, 447 (2019).

[4] T. Li and F. Yang: Phys. Rev. B **81**, 214509 (2010).

[5] For example, K. Ido, *et al.*: Phys. Rev. B **101**, 075124 (2020).

[6] A. V. Knyazev: SIAM J. Sci. Comput. **23**, 517 (2001).

[7] T. Sakurai and H. Sugiura: J. Comput. Appl. Math. **159**, 119 (2003).

Many-body topological phases in strongly correlated electron systems

Kota IDO

Institute for Solid State Physics,

The University of Tokyo, Kashiwa-no-ha, Kashiwa, Chiba 277-8581

The Kondo lattice model is one of the fundamental models for strongly correlated electron systems [1]. This model has been originally considered an effective model for heavy fermion systems, but recently, for van der Waals heterostructure systems [2]. In this model, the competition between the RKKY magnetic effective interaction and the formation of the Kondo singlet gives birth to enriched intriguing states such as the Kondo insulator, non-Fermi liquids, and exotic superconducting states.

As one of them, the magnetic topological insulator has been discussed in the last decade [3-5]. Previous studies mentioned that the magnetic topological insulator stabilizes as the ground state at quarter filling in the classical limit [4] or within spin-wave approximation [5]. However, the role of quantum effects beyond the spin-wave approximation, including the formation of the Kondo singlet, is still an enigmatic problem.

In this study [6], we investigate the ground states of the spin 1/2 Kondo lattice model on the triangular lattice at quarter filling. As a quantum many-body solver, we employ the variational Monte Carlo (VMC) method [7]. We find that a noncoplanar magnetic ordered state becomes the ground state in the intermediate coupling region. To identify the topological property of the ground states, we propose an efficient VMC method for calculating the many-body Chern number based on Resta's polarization approach [8,9]. Using this method, we find that the noncoplanar magnetic state has indeed the non-trivial many-body Chern number. Our results shed light on not only a further pathway to realize correlated magnetic topological insulators but also an efficient analysis of the many-body topological states in strongly correlated electron systems.

References

[1] H. Tsunetsugu, M. Sigrist, and K. Ueda, Rev. Mod. Phys. **69** 809 (1997).

[2] V. Vaňo, et al., Nature **599**, 582 (2021).

[3] I. Martin and C. D. Batista, Phys. Rev. Lett. **101** 156402 (2008).

[4] Y. Akagi and Y. Motome, J. Phys. Soc. Jpn. **79** 083711 (2010).

[5] Y. Akagi, M. Udagawa, and Y. Motome, J. Phys. Soc. Jpn. **82** 123709 (2013).

[6] K. Ido and T. Misawa, arXiv:2310.07094.

[7] T. Misawa et al., Comput. Phys. Commun. **235** 447 (2019).

[8] R. Resta, Phys. Rev. Lett. **80** 1800 (1998).

[9] B. Kang, W. Lee, and G. Y. Cho, Phys. Rev. Lett. **126** 016402 (2021).

Magnetically ordered states on the hexagonal quasiperiodic tilings

Akihisa Koga
Department of Physics, Tokyo Institute of Technology, Meguro, Tokyo 152-8551

Quasiperiodic systems have attracted considerable interest since the discovery of the Al-Mn quasicrystal. Recently, electron correlations in quasicrystals have been actively studied after quantum critical behavior was observed in the Au-Al-Yb quasicrystal. In addition, long-range ordered states have been reported such as superconductivity in the Al-Zn-Mg quasicrystal, and ferromagnetically ordered states in the Au-Ga-R (R = Gd, Tb, Dy) quasicrystals. These studies have stimulated theoretical investigations on electron correlations and the spontaneously symmetry breaking states in quasicrystals.

We have introduced golden-mean hexagonal and trigonal quasiperiodic tilings, using a generalization of de Bruijn's grid method [1]. In this work, we have demonstrated the structural properties and substitution rules of the H_{00} and $H_{\frac{1}{2}\frac{1}{2}}$ tilings, where the subscript refers to the tunable grid-shift parameters. These structural properties are distinct from those for the Penrose, Ammann-Beenker, and Socolar tilings. One of the important points is the existence of the sublattice imbalance. However, they are still rooted in the physical world of experimentally observed trigonal and hexagonal quasiperiodic systems. It is therefore desirable to study magnetic properties on quasiperiodic systems with sublattice imbalances.

In this project, we have clarified magnetic properties of the Hubbard model on the H_{00} and $H_{\frac{1}{2}\frac{1}{2}}$ tilings and have studied the macroscopically degenerate states with $E = 0$ in the tight-binding model, which should play an important role for magnetic properties in the weak coupling limit [2, 3, 4]. We have clarified that two extended states appear in one of the sublattices, while confined states appear in the other. Furthermore, we have obtained the fraction of the confined states in terms of Lieb's theorem, considering magnetism in the weak coupling limit. We also have discussed how magnetic properties are affected by electron correlations in the half-filled Hubbard model.

References

[1] S. Coates, A. Koga, T. Matsubara, R. Tamura, H. R. Sharma, R. McGrath, and R. Lifshitz, arXiv:2201.11848.

[2] A. Koga and S. Coates, *Phys. Rev. B* **105**, 104410 (2022).

[3] T. Matsubara, A. Koga, and S. Coates, *J. Phys.: Conf. Ser.* **2461**, 012003 (2023).

[4] T. Matsubara, A. Koga, and S. Coates, *Phys. Rev. B* **109**, 014413 (2024).

Magnetic-field control of non-Abelian anyons in Kitaev quantum spin liquids

Joji NASU
Department of Physics, Tohoku University
Sendai 980-8578

The Kitaev model has been widely studied as a quantum many-body model that possesses a quantum spin liquid in its ground state [1], and a proposal for realizing this model in transition metal compounds has been made [2]. In this model, elementary excitations behave as if a spin is split into two independent quasiparticles: a Majorana fermion and a vison. Moreover, when a magnetic field is applied, each vison is accompanied by Majorana zero modes, leading to non-Abelian anyons. These non-Abelian anyons are potential computational elements in topological quantum computing, and thus, theoretical proposals for their temporal and spatial control are highly needed. However, observing, generating, and controlling these quasiparticles remain challenging. In this research project, we investigate the real-time dynamics of quasiparticles in the Kitaev quantum spin liquid in large clusters to clarify how to control visons with Majorana zero modes.

In the present study, we calculate the time evolution of the Kitaev quantum spin liquid in the presence of an excited vison using time-dependent mean-field theory. In this method, time evolution is computed based on the von Neumann equation for a time-dependent density matrix [3, 4]. To evaluate the commutation relations between the Hamiltonian and density matrices, we use the MKL library with thread parallelization. This approach is effective for computations involving larger matrices, which are required in the present real-space calculations with larger lattice clusters.

We apply the time-dependent local magnetic field to an excited vison and calculate the time evolution of the system. We find that a vison can follow a local field sweeping through the system. We also confirm that a Majorana zero mode always accompanies the vison even while it moves by following a time-dependent local field [5]. We reveal optimal conditions for the local field to control a non-Abelian anyon, which is determined by interactions between the fractional quasiparticles of the Kitaev model. Furthermore, we demonstrate creating and annihilating visons by applying local magnetic fields in addition to vison manipulations.

References

[1] A. Kitaev, , Ann. Phys. (NY) **303**, 2 (2003).

[2] G. Jackeli and G. Khaliullin, Phys. Rev. Lett. **102**, 017205 (2009).

[3] J. Nasu, and Y. Motome, Phys. Rev. Research **1**, 033007 (2019).

[4] T. Minakawa, Y. Murakami, A. Koga, and J. Nasu, Phys. Rev. Lett. **125**, 047204 (2020).

[5] C. Harada, A. Ono, and J. Nasu, Phys. Rev. B **108**, L241118 (2023).

Electronic and phonon states and superconductivity of multi-band low-carrier systems based on first-principles and quantum many-body calculations

Yoshiaki ŌNO

Department of Physics,

Niigata University, Ikarashi, Niigata 950-2181

We have studied the effects of ionizations induced by proton and ^{12}C radiation and molecular conformational changes in DNA. This year, we calculated the stable structure, band dispersion, and wave function of DNA under the condition that one and two electrons per 10 base pairs are ionized by radiation corresponding to 10 and 20 percent hole doped cases using the first-principles calculation software OpenMX and discussed the relationship between the energy dependence of each incident radiation type and the molecular conformational change of DNA [1].

We have also studied the superconductivity in the two-band Hubbard model (so-called *d-p* model) on the basis of the dynamical mean-field theory (DMFT), in which the irreducible vertex function Γ has no k-dependence and then only the s-wave superconductivities with the spin-singlet even-frequency pairing and the spin-triplet odd-frequency pairing are possibly realized. In the previous DMFT studies, both the singlet and triplet superconductivities have not been observed in the one-band Hubbard model. On the other hand, in the two-band Hubbard model, the singlet and/or triplet superconductivities have been found to be realized. However, the explicit results of the pair (superconducting) susceptibilities which show divergence as the temperature approaches the superconducting transition temperature T_c were not shown there. This year, we calculated the singlet and triplet pair susceptibilities by solving the Bethe-Salpeter equation and determine T_c in the two-band Hubbard model on a Bethe lattice with infinite connectivity. We obtained the phase diagrams of T_c for the singlet and triplet superconductivities as functions of doping, on-site Coulomb interaction and charge-transfer energy [2].

References

[1] T. Sekikawa, Y. Matsuya, B. Hwang, M. Ishizaka, H. Kawai, Y. Ōno, T. Sato, and T. Kai, Nucl. Instrum. Methods Phys. Res. B **548**, 165231 (2024).

[2] Y. Inokuma, and Y. Ōno, J. Phys. Soc. Jpn. **93**, 043701 (2024).

Designing and evaluating quantum many-body chaos

Masaki TEZUKA

Department of Physics, Kyoto University, Kitashirakawa, Sakyo-ku, Kyoto 606-8502

The Sachdev-Ye-Kitaev (SYK) model is a model of fermions with independently random all-to-all four-point interactions obeying the Gaussian distribution. The model can be solved in the sense of random coupling average in the limit of large number of fermions, and the Lyapunov exponent, defined by the out-of-time ordered correlation functions, realizes the universal upper bound at low temperatures.

Previously, we studied a "sparse" version of the SYK model, in which the number of non-zero interaction terms is reduced to the order of the number of fermions. While it had been known that the sparse model reproduces essential features of the original SYK model for Gaussian random couplings [1], we analyzed the spectral statistics of a further simplification, in which the magnitude of the nonzero couplings is set to be a constant [2]. This simplification is an improvement in the sense that the spectral correlation is stronger and thus closer to the random-matrix universality for the same number of non-zero couplings, compared to the Gaussian random case.

Towards quantum simulation of such models, we considered another simplification of the SYK model: a model of Pauli spin operators with all-to-all 4-local interactions, obtained by replacing Majorana fermions in the SYK model with spin operators. From the numerical analysis using the ISSP Supercomputer, we observed a striking quantitative coincidence between this spin model and the SYK model, which suggests that this spin model is strongly chaotic [3].

We also studied the quantum error correction (QEC) capabilities of the unitary time evolution according to various time-independent Hamiltonians by the Hayden-Preskill protocol. An unknown quantum state thrown into a quantum many-body system can or cannot be decoded, with the knowledge of the initial state of the system and the time evolution, by accessing only a part of the system after time evolution, depending on whether the Hamiltonian of the system is scrambling the quantum information. We compared the error estimate, obtained by the decoupling approach, against the one for random unitary evolutions obeying the circular unitary (Haar) ensemble. For the sparse SYK model, the QEC error estimate approaches the Haar value within a short time if the spectral statistics is random-matrix like. In the presence of two-fermion interactions, departure from the Haar value is observed before the Fock space localization. On the other hand, for quantum spin chains often studied in the context of chaotic dynamics, scrambling is not observed in this sense and the QEC error estimate remains large in the long-time limit [4].

References

[1] S. Su *et al.*, arXiv:2008.02303; A. M. Garcia-Garcia *et al.*, Phys. Rev. D **103**, 106002 (2021).

[2] M. Tezuka, O. Oktay, E. Rinaldi, M. Hanada, and F. Nori, Phys. Rev. B **107**, L081103 (2023).

[3] M. Hanada, A. Jevicki, X. Liu, E. Rinaldi, and M. Tezuka, J. High Energ. Phys. in press (arXiv:2309.15349).

[4] Y. Nakata and M. Tezuka, Phys. Rev. Research **6**, L022021 (2024).

Magnetization plateau and anomaly induced by spin-lattice coupling in pyrochlore antiferromagnets

Hidemaro SUWA
Department of Physics, University of Tokyo, Tokyo 113-0033

Frustrated magnetic systems inherently exhibit macroscopic degeneracy, which can be lifted by various perturbations, leading to diverse magnetic phenomena. Among these, spin-lattice coupling plays a pivotal role in stabilizing magnetization plateaus, particularly in spinel magnetic compounds. In this context, lattice modes intertwined with spin degrees of freedom are effectively modeled using simplified phonon approaches. Here, bond phonons encapsulate magnetostriction effects resulting from spin-lattice interactions, whereas site phonons are instrumental in elucidating the long-range magnetic order of real materials.

Despite their utility, these models fall short in fully accounting for the behaviors observed in certain systems, such as chromium spinel oxides that manifest pyrochlore antiferromagnetic properties. Although bond and site phonon models successfully reproduce the experimentally observed half-magnetization plateau in pyrochlore systems, they fail to capture the high-field magnetization anomaly prevalent in many chromium spinel oxides, which is arguably considered an indicator of potential magnon-bound states.

To address these discrepancies and enhance our understanding of the magnetization process in chromium spinel oxides and other related frustrated systems, a more sophisticated spin-lattice model is necessary. Our research adopts a combined spin-lattice model that amalgamates both bond and site-phonon effects. By tracing out lattice degrees of freedom, we derive an effective spin model that includes higher-order interactions, such as biquadratic and three-body spin interactions. This model introduces an additional parameter representing the relative contributions from bond and site phonons, aiming to provide a more accurate depiction of experimental observations, including magnetostriction, long-range magnetic order, and specific heat behavior.

Using the Monte Carlo method, enhanced by an advanced update scheme[1], we examined the proposed spin-lattice model within a pyrochlore lattice framework. The simulations were performed on ISSP System B in the class C project (2023-Ca-0112) in an MPI parallel computation using up to eight nodes simultaneously. Our simulations, calibrated with optimal parameters for various chromium spinel oxides, successfully replicate the half-magnetization plateau and specific heat measurements. Moreover, the model predicts a magnetization anomaly under high magnetic field conditions, suggesting a complex magnetic ordering not previously found. Our findings offer a novel perspective on the high-field magnetic anomaly and contribute to a broader understanding of the pyrochlore antiferromagnet.

References

[1] M. Gen and H. Suwa, Phys. Rev. B **105**, 174424 (2022).

Phtoinduced transient absorption spectrum in two-leg-ladder Mott insulator with strong dimer correlation

Takami TOHYAMA
Department of Applied Physics, Tokyo University of Science, Katsushika, Tokyo 125-8585

Photoinduced nonequilibrium states in the Mott insulators reflect the fundamental nature of competition between itinerancy and localization of the charge degrees of freedom. The spin degrees of freedom will also contribute to the competition in a different manner depending on lattice geometry. There is a spin gap in a two-leg-ladder Mott insulator. The spin gap is ascribed to an energy to break spin-singlet dimer predominately formed along the rung. Because of spin dimer formation, dimer-dimer correlation is also strong. Under the presence of dimer-dimer correlation, photoexcited doublon and holon tend to form a localized exciton not to break spin dimers. Such localized exciton formation appears in optical absorption as a large peak at a high frequency slightly above the on-site Coulomb energy [1]. Therefore, it is interesting to clarify how the localized exciton contributes to photoexcitation.

To answer this question, in this project we investigate pulse-excited states of the half-filled two-leg Hubbard ladder using the time-dependent density-matrix renormalization group (tDMRG) and time-dependent exact diagonalization (tED) based on the Lanczos technique [2]. Our tDMRG makes use of the Legendre polynomial for the calculation of time-evolution operator. We use two target states at a given time t and $t + \Delta t$ to construct a basis set that can express wavefunctions in the time-dependent Hilbert space. With the two-target tDMRG procedure, we can calculate time-dependent physical quantities with high accuracy even when the Hamiltonian varies rapidly with time.

From our tDMRG and tED simulations, we find that strong monocycle pulse inducing quantum tunneling gives rise to anomalous suppression of photoinduced in-gap weight, leading to negative weight [2]. This is in contrast to finite positive weight in an extended Hubbard chain [3]. Examining multipulse pumping for states above the Mott gap, we attribute the origin of this anomalous behavior of in-gap spectral weight to photoinduced localized exciton that reflects strong spin-singlet dimer correlation in the ground state. We note that so-called Majumdar-Ghosh chain having single-dimer ground state does not show in-gap negative weight.

This contrasting behavior can be confirmed if one applies a monocycle terahertz pulse to a one-dimensional Mott insulator such as Sr_2CuO_3 and a two-leg ladder Mott insulator such as $La_6Ca_8Cu_{24}O_{41}$, increases pulse strength, and observes how in-gap weight evolves with the strength.

References

[1] K. Shinjo, Y. Tamaki, S. Sota, and T. Tohyama: Phys. Rev. B **104**, 205123 (2021).

[2] T. Tohyama, K. Shinjo, S. Sota, and S. Yunoki, Phys. Rev. B **108**, 035113 (2023).

[3] K. Shinjo, S. Sota, and T. Tohyama: Phys. Rev. Res. **4**, L032019 (2022).

Nonlinear response in correlated materials

Robert PETERS

Department of Physics,

Kyoto University, Kyoto, 606-8502

The research on nonlinear phenomena in correlated materials advanced in two stages. On the one hand, (1) we analyzed the nonlinear Edelstein effect in correlated materials using a perturbative technique, and (2) we made significant progress in analyzing responses using time evolution. On the other, we (3) were able to calculate the time evolution of a quantum skyrmion driven by a magnetic field gradient using neural networks.

1) We developed a method to study the nonlinear spin response using single-particle Green's functions. We then explored the effect of correlations on this nonlinear Edelstein effect using the dynamical mean-field approximation. We found that correlations can enhance the effect in static electric fields. We also explored the optical version of the effect, i.e., the build-up of a static spin polarization in a time-dependent electric field, and we identified a delicate interplay between the lifetime of excitations and renormalization that can enhance or suppress the Edelstein effect. [1]

(2) We studied the non-equilibrium dynamics of correlated systems and analyzed the response to an external electric field. Here, we perturbatively included fluctuations in the calculations using a correlation expansion. We demonstrated that for a noninteracting system, the Green's function technique mentioned above and the time evolution yield identical results. Then, we demonstrated in an interacting Rice-Mele model that the biexciton transition strongly enhances the response whenever the frequency of the incident light matches the exciton energy. [2]

(3) We used neural network quantum states on ISSP's GPU to calculate the time-dependent wave function of a large two-dimensional quantum spin model hosting quantum skyrmions. We demonstrated that the quantum skyrmion is driven by a magnetic field gradient. We furthermore observed the merging of two quantum

skyrmions through the formation of an exceptional spin configuration. This merging is accompanied by a large build-up of entanglement. [3]

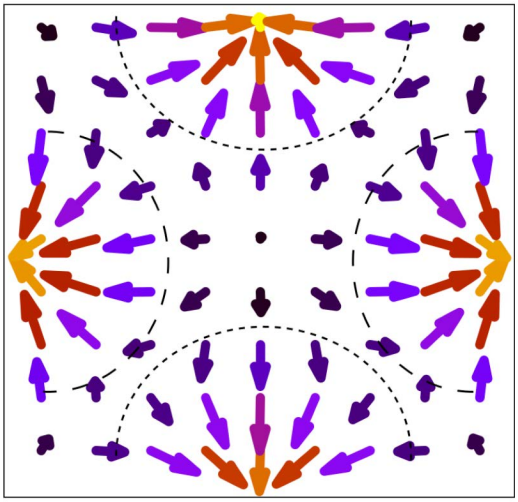

Figure 1:Ground state with two quantum as calculated by neural network quantum states

References

[1] "Nonlinear Edelstein Effect in Strongly Correlated Electron Systems" Jun Ōiké, Robert Peters; arXiv:2403.17189

[2] "Two-particle correlation effects on nonlinear optical responses in the one-dimensional interacting Rice-Mele model" Akira Kofuji and Robert Petersl Phys. Rev. B 109, 155111

[3] "Quantum skyrmion dynamics studied by neural network quantum states" Ashish Joshi, Robert Peters, Thore Posske; arXiv:2403.08184

Research of Three-Channel Kondo Effect Emerging from Tb and Tm Ions

Takashi HOTTA
Department of Physics, Tokyo Metropolitan University
1-1 Minami-Osawa, Hachioji, Tokyo 192-0397

Inspired by the discovery of three-channel Kondo effect emerging from Ho ions for the case of Γ_5 triplet ground state [**?**], we have attempted to find the three-channel Kondo effect also from Tb and Tm ions for the same case of the Γ_5 triplet ground state.

First let us explain the model Hamiltonian. It is convenient to define one f-electron state by the eigenstate of spin-orbit and crystalline electric field (CEF) potential terms. We find Γ_7 doublet and Γ_8 quartet from $j=5/2$ sextet whereas we find Γ_6 doublet, Γ_7 doublet, and Γ_8 quartet from $j=7/2$ octet under the cubic CEF potential. Then, we include the Γ_7 and Γ_8 conduction electron bands. Note that we consider only the hybridization between the conduction and $j=7/2$ electrons. The model Hamiltonian is given by

$$\begin{aligned} H &= \sum_{\boldsymbol{k},\mu,\tau} \varepsilon_{\boldsymbol{k}} c^\dagger_{\boldsymbol{k}\mu\tau} c_{\boldsymbol{k}\mu\tau} + \sum_{\boldsymbol{k},\mu,\tau} V(c^\dagger_{\boldsymbol{k}\mu\tau} f_{b\mu\tau} + \text{h.c.}) \\ &+ nE_f + \sum_{j,\mu,\tau} (\lambda_j + B_{j,\mu}) f^\dagger_{j\mu\tau} f_{j\mu\tau} \\ &+ \sum_{j_1\sim j_4} \sum_{\mu_1\sim\mu_4} \sum_{\tau_1\sim\tau_4} I^{j_1 j_2, j_3 j_4}_{\mu_1\tau_1\mu_2\tau_2,\mu_3\tau_3\mu_4\tau_4} \\ &\times f^\dagger_{j_1\mu_1\tau_1} f^\dagger_{j_2\mu_2\tau_2} f_{j_3\mu_3\tau_3} f_{j_4\mu_4\tau_4}, \end{aligned} \tag{1}$$

where $\varepsilon_{\boldsymbol{k}}$ is the dispersion of conduction electron with wave vector $\boldsymbol{k}$, $c_{\boldsymbol{k}\mu\tau}$ is the annihilation operator of a conduction electron, $f_{j\mu\tau}$ is the annihilation operator of a localized f electron in the bases of (j,μ,τ), j is the total angular momentum, $j=5/2$ and $7/2$ are denoted by "a" and "b", respectively, μ distinguishes the cubic irreducible representation, Γ_8 states are distinguished by $\mu=\alpha$ and β, while the Γ_7 and Γ_6 states are labeled by $\mu=\gamma$ and δ, respectively, τ denotes the pseudo-spin, which distinguishes the degeneracy concerning the time-reversal symmetry, V denotes the hybridization between f electron in the μ orbital and conduction electron of the μ band, n is the local f-electron number at an impurity site, and E_f is the f-electron level to control n.

As for the spin-orbit term, we obtain $\lambda_a = -2\lambda$ and $\lambda_b = (3/2)\lambda$, where λ is the spin-orbit coupling of f electron. We set $\lambda = 0.212$ and 0.326 eV for Tb and Tm ions, respectively. Concerning the CEF potential term for $j=5/2$, we obtain $B_{a,\alpha} = B_{a,\beta} = 1320B^0_4/7$ and $B_{a,\gamma} = -2640B^0_4/7$, where B^0_4 denotes the fourth-order CEF parameter for the angular momentum $\ell=3$. For $j=7/2$, we obtain $B_{b,\alpha} = B_{b,\beta} = 360B^0_4/7 + 2880B^0_6$, $B_{b,\gamma} = -3240B^0_4/7 - 2160B^0_6$, and $B_{b,\delta} = 360B^0_4 - 3600B^0_6/7$. In the following calculations, we use the parametrization as $B^0_4 = Wx/15$ and $B^0_6 = W(1-|x|)/180$ for $\ell=3$, where x specifies the CEF scheme for the $O_{\rm h}$ point group, while W determines the energy scale of the CEF potentials. In this work, we set $W = 10^{-3}$ eV and treat x as the parameter to control the CEF ground state.

For the Coulomb interaction terms, we do not show the explicit forms of I here, but they are expressed by the four Slater-Condon parameters, F^0, F^2, F^4, and F^6. These values should be determined from experimental results, but here we simply set the ratio as

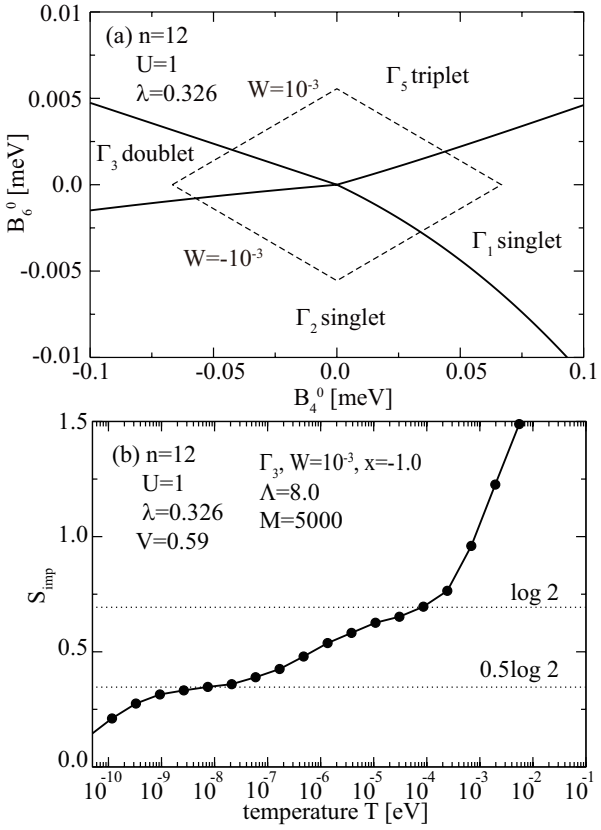

Figure 1: (a) Local CEF ground-state phase diagram on the (B_4^0, B_6^0) plane for $n = 12$ with $U = 1$ and $\lambda = 0.326$. The dashed rhombus denotes the trajectory of $B_4^0 = Wx/15$ and $B_6^0 = W(1 - |x|)/180$ for $-1 \le x \le 1$ with $W = \pm 10^{-3}$. (b) Entropy vs. temperature for $x = -1$, $W = 10^{-3}$, and $V = 0.59$ for the case with the local Γ_3 ground state.

$F^0/10 = F^2/5 = F^4/3 = F^6 = U$, where U indicates the Hund's rule interaction among the f orbitals. In this work, we set $U = 1$ eV.

In the present report, we show only the results for the Tm ion. Results for the Tb ion will be shown elsewhere. First we consider the local CEF ground-state phase diagram for $n = 12$. The ground-state multiplet for $B_4^0 = B_6^0 = 0$ is characterized by the total angular momentum $J = 6$. Under the cubic CEF potentials, the tre-dectet of $J = 6$ is split into four groups as one Γ_1 singlet, one Γ_2 singlet, one Γ_3 doublet, one Γ_4 triplet, and two Γ_5 triplets. Then, we obtain four kinds of local ground states for $n = 12$, as shown in Fig. 1(a). Roughly speaking, the Γ_5 triplet appears widely for $B_6^0 > 0$, whereas the Γ_2 singlet is found for $B_6^0 < 0$. In the region of $B_6^0 \approx 0$ and $B_4^0 > 0$, the Γ_1 singlet is stabilized. For $B_4^0 < 0$, we find the Γ_3 doublet.

The three-band Anderson model is analyzed with the use of a numerical renormalization group (NRG) method. We introduce a cut-off Λ for the logarithmic discretization of the conduction band. Due to the limitation of computer resources, we keep M low-energy states. Here we use $\Lambda = 8$ and $M = 5,000$. In the NRG calculation, the temperature T is defined as $T = D\Lambda^{-(N-1)/2}$, where D is half the conduction band width, which is set as 1 eV, and N is the number of renormalization steps.

The appearance of the three-channel Kondo effect from Ho ion is characterized by a residual entropy $S_{\rm imp}$ of $\log \phi$ with the golden ratio $\phi = (1 + \sqrt{5})/2$ for the local Γ_5 triplet ground state [**?**]. Thus, we have tried to find the residual entropy $\log \phi$ from the Tm ion in the parameter space corresponding to the local Γ_5 triplet ground state, but we could not find any signals of $\log \phi$ for the case of $n = 12$. It is inevitable to conclude that the three-channel Kondo effect does not appear for the Tm ion.

However, it is interesting to report the discovery of $S_{\rm imp} = \log \sqrt{2}$, which is characteristic of the two-channel Kondo effect. In Fig. 1(b), we show the f-electron entropy for $x = -1$, $W = 10^{-3}$, and $V = 0.59$. In this figure, we find the signal of the residual entropy of $\log \sqrt{2}$, although we did not perform the fine tuning of the CEF parameters to obtain the residual entropy even at extremely low temperatures. Thus, we conclude that for the case of $n = 12$, the two-channel Kondo effect is found even in the three-band Anderson model.

References

[1] T. Hotta, J. Phys. Soc. Jpn. **90**, 113701 (2021).

Studies on unconventional superconductivity in multilayer nickelates

KAZUHIKO KUROKI
Department of Physics, Osaka University
1-1 Machikaneyama, Toyonaka, Osaka, 560-0043, Japan

Several studies in the past have shown that the superconducting T_c in the bilayer Hubbard model can be higher than that of the d-wave superconducting state in the single-orbital Hubbard model [1, 2]. Therefore, realizing the bilayer Hubbard model in actual materials can be considered as a path toward finding new high temperature superconductors. The present author proposed that a double layer Ruddlesden-Popper compound $La_3Ni_2O_7$ can be a good candidate for realizing the bilayer Hubbard model that satisfies the above-mentioned conditions [3]. In this material, for which the Ni $3d$ electron configuration is $d^{7.5}$, the $3d_{3z^2-r^2}$ orbitals are elongated in the z (out-of-plane) direction so that $t_\perp$ between the layers is much larger than the in-plane hoppings between the neighboring $d_{3z^2-r^2}$ orbitals, and also the $d_{3z^2-r^2}$ orbitals are nearly half-filled. Hence the $d_{3z^2-r^2}$ portion of the electronic structure appears to be favorable for superconductivity from the above-mentioned viewpoint of the bilayer model, although deviation from the ideal model arises due to the presence of the Ni $3d_{x^2-y^2}$ bands, which are nearly quarter-filled, overlapping and hybridizing with the $d_{3z^2-r^2}$ bands. In this context, a recent experimental finding that $La_3Ni_2O_7$ exhibits high T_c superconductivity with a highest T_c of about 80 K under pressure above 14 GPa [4] is certainly intriguing.

Inspired by this experiment, we theoretically revisited the possibility of superconductivity in $La_3Ni_2O_7$ by constructing a four-orbital model that takes into account the crystal structure at high pressures, and applying fluctuation exchange approximation to the model. We find that $s\pm$-pairing superconductivity, which is somewhat similar to that of the bilayer Hubbard model, can take place with high T_c that is consistent with the experimental observation[6].

We have also performed density matrix renormalization group studies in a two-orbital Hubbard[7] and t-J ladder[8] models that mimic the electronic state of $La_3Ni_2O_7$. Our calculation shows that both the interchain, intraorbital pair correlation within both $d_{3z^2-r^2}$ and $3d_{x^2-y^2}$ orbitals exhibit slow, power law decay, which are enhanced by both the interlayer coupling and Hund's coupling. More interestingly, the interorbital pair correlation also exhibits a slow decay comparable to the intraorbital ones, and this occurs even in the absence of Hund's coupling, for which the pairing glue mediated by Hund's coupling is absent.

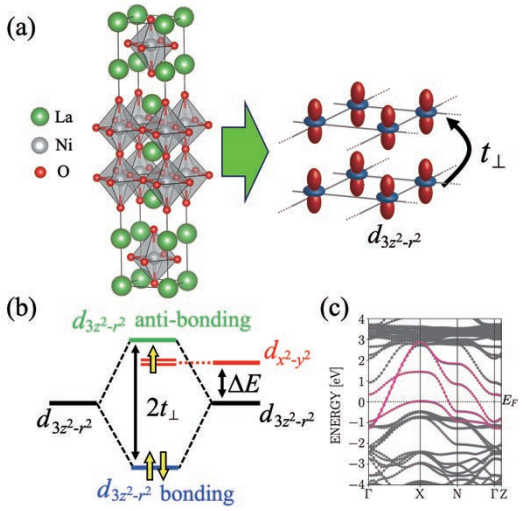

FIG. 1. (a)Crystal structure drawn by VESTA [5], (b)an energy diagram of e_g orbitals in our bilayer model, and (c) the first-principles band structure of $La_3Ni_2O_7$ are shown. In the right side of panel (a), schematic figure of the bilayer model of the $d_{3z^2-r^2}$ orbitals is depicted. In the panel (c), Wannier-interpolated band structure (pink lines) of the four-orbital model is superposed on the first-principles band structure (grey lines). The definition of the energy level offset ΔE and $t_\perp$, key parameters of this study, are indicated in the panel (b) and (a), respectively.

Following the study on the bilayer $La_3Ni_2O_7$, we further studied the possibility of superconductivity in a trilayer Ruddlesden-Popper nickelate $La_4Ni_3O_{10}$ under pressure. Through DFT calculations, we found that a structural phase transition from monoclinic to tetragonal takes place around 15 GPa. Using the tetragonal crystal structure, we have theoretically investigated the possibility of superconductivity, where a combination of fluctuation exchange approximation and linearized Eliashberg equation is applied to a six-orbital model constructed from first principles band calculation. The obtained results suggests that $La_4Ni_3O_{10}$ may also become superconducting under high pressure with T_c comparable to relatively low T_c cuprates, although it is not as high as $La_3Ni_2O_7$[9]. This theoretical expectation was confirmed from experiments on polycrystalline samples[9].

[1] K. Kuroki, T. Kimura, and R. Arita, Phys. Rev. B **66**, 184508 (2002).
[2] V. Mishra, D. J. Scalapino, and T. A. Maier, Sci. Rep. **6**, 32078 (2016).
[3] M. Nakata, D. Ogura, H. Usui, and K. Kuroki, Phys. Rev. B **95**, 214509 (2017).
[4] H. Sun, M. Huo, X. Hu, J. Li, Z. Liu, Y. Han, L. Tang, Z. Mao, P. Yang, B. Wang, J. Cheng, D.-X. Yao, G.-M. Zhang, and M. Wang, Nature (2023).
[5] K. Momma and F. Izumi, J. Appl. Crystallogr. **44**, 1272 (2011).
[6] H. Sakakibara, N. Kitamine, M. Ochi, and K. Kuroki, Phys. Rev. Lett. **132**, 106002 (2024).
[7] T. Kaneko, H. Sakakibara, M. Ochi, and K. Kuroki, Phys. Rev. B **109**, 045154 (2024).
[8] M. Kakoi, T. Kaneko, H. Sakakibara, M. Ochi, and K. Kuroki, (2023), arXiv:2312.04304.
[9] H. Sakakibara, M. Ochi, H. Nagata, Y. Ueki, H. Sakurai, R. Matsumoto, K. Terashima, K. Hirose, H. Ohta, M. Kato, Y. Takano, and K. Kuroki, Phys. Rev. B **109**, 144511 (2024).

Theoretical Study for Mixed-sequence Oligomer Salt Modeling Doped PEDOT Family

Tomoko FUJINO

Institute for Solid State Physics,

The University of Tokyo, Kashiwa-no-ha, Kashiwa, Chiba 277-8581

Organic conductors are divided into two categories: low-molecular-weight and polymer-based materials. Low-molecular-weight materials have well-defined structures but limited control over conductivities. Conductive polymers, on the other hand, have highly conjugated systems but are difficult to control due to their structural inhomogeneity.

To bridge this gap, oligomer-based conductors were developed as intermediate materials. These conductors are made of oligo(3,4-ethylenedioxythiophene), oligoEDOT, and are modeled after the doped PEDOT family 1–4]. The conductivities of these materials were studied by considering counter anion variations, lengths of oligomer donor, and band fillings. Through the study, oligoEDOT analogs were developed with tunable room temperature conductivities by several orders of magnitude, including a metallic state above room temperature [4]. The electronic structural insights were evaluated by first-principles calculations (QUANTUM ESPRESSO, RESPACK, and H-wave packages; Ohtaka, Supercomputer center, ISSP), and it was revealed that the range of Coulomb repulsion between carriers, $\boldsymbol{U}_{\mathbf{eff}}$, is the dominant factor that determines the relationship between the structures and conductivities [5]. The oligoEDOT conductor systems have a unique feature of widely variable $\boldsymbol{U}_{\mathbf{eff}}$, differentiating these systems from strongly electron-correlated systems.

References

[1] R. Kameyama, T. Fujino*, S. Dekura, M. Kawamura, T. Ozaki, and H. Mori*, Chem. Eur. J. **27**, 6696 (2021).

[2] R. Kameyama, T. Fujino,* S. Dekura, and H. Mori,* Phys. Chem. Chem. Phys. **24**, 9130 (2022).

[3] R. Kameyama, T. Fujino, S. Dekura, S. Imajo, T. Miyamoto, H. Okamoto, H. and Mori,* J. Mater. Chem. C **10** (9), 7543 (2022).

[4] K. Onozuka, T. Fujino,* R. Kameyama, S. Dekura, K. Yoshimi, T. Nakamura, T. Miyamoto, T. Yamakawa, H. Okamoto, H. Sato, T. Ozaki, and H. Mori,* J. Am. Chem. Soc. **145**, 15152 (2023).

[5] T. Fujino,* R. Kameyama, K. Onozuka, K. Matsuo, S. Dekura, K. Yoshimi, and H. Mori,* Faraday Discuss. **250**, 348 (2024).

Analyses of magnetic properties in the Hubbard models.

Atsushi Yamada
Department of Physics, Chiba University
Chiba 263-8522, Japana, Chiba 277-8581

Exotic states like a spin liquid state has attracted a lot of interest. Foe example, spin liquid may be realized in geometrically frustrated systems like the charge organic transfer salts κ-(BEDT-TTF)$_2$X[1] and Cs_2CuCl_4.[2] Hubbard model on the an-isotropic triangular lattice is a simple theoretical model of these compounds. Some theoretical groups, including us have studied that model, and idntified a possible candidates of spin liquid state in this model.[3, 4] A spin liquid could arise also in the intermediate coupling region of strongly correlated systems between a semimetal and ordered state, because in this case a correlation-driven insulating gap might open before the system becomes ordered. This possibility might be realized in the half-filled Hubbard model on the honeycomb lattice, where a semi-metal is realized at $U = 0$.

We have studied the magnetic and metal-to-insulator transitions in this model by variational cluster approximation.[6] The 10-site and 16-site clusters are used in our study as a reference system. Parts of numerical calculations were done using the computer facilities of the ISSP. Our results rule out the existence of the spin liquid in this model. Our results agree with recent large scale Quantum Monte Carlo simulations.[5]

We are currently improving our program using MPI technique so that we will be able to study a larger cluster size system compared to our previous studies[4] and more memory-intensive states like superconductivity.

References

[1] Y. Shimizu, K. Miyagawa, K. Kanoda, M. Maesato, and G. Saito, Phys. Rev. Lett. **91**, 107001 (2003); Y. Kurosaki, Y. Shimizu, K. Miyagawa, K. Kanoda, and G. Saito, Phys. Rev. Lett. **95**, 177001 (2005).

[2] R. Coldea, D.A. Tennant, A.M. Tsvelik, and Z. Tylczynski, Phys. Rev. Lett. **86**, 1335 (2001); R. Coldea, D.A. Tennant, and Z. Tylczynski, Phys. Rev. Lett. **68**, 134424 (2003).

[3] T. Yoshioka, A. Koga, and N. Kawakami, Phys. Rev. Lett. **103**, 036401 (2009); P. Sahebsara and D. Sénéchal, Phys. Rev. Lett. **100**, 136402 (2008); L.F. Tocchio, H. Feldner, F. Becca, R. Valenti, and C. Gros, Phys. Rev. B **87**, 035143 (2013); L.F. Tocchio, C. Gros, R. Valentí, F. Becca, Phys. Rev. B **89**, 235107 (2014).

[4] A. Yamada, Phys. Rev. B **89**, 195108 (2014); Phys. Rev. B **90**, 235138 (2014).

[5] S. Sorella, Y. Otsuka, and S. Yunoki, Sci. Rep. **2**, 992 (2012); F. F. Assaad and I. F. Herbut, Phys. Rev. X **3**, 031010 (2013); F. Parisen Toldin, M. Hohenadler, F. F. Assaad, and I. F. Herbut, Phys. Rev. B **91**, 165108 (2015).

[6] A. Yamada, Int. J. Mod. Phys. B **30**, 1650158 (2016).

Stripes and Charge-ordered ground state and its coexistence with superconductivity in correlated electron systems

Takashi YANAGISAWA
National Institute of Advanced Industrial Science and Technology (AIST)
1-1-1 Umezono, Tsukuba, Ibaraki 305-8568, Japan

1 Introduction

Our numerical research is based on the optimized variational Monte Carlo method[1]. We use the optimized many-body wave function which is improved by multiplying by off-diagonal exponential operators given by $e^{-\lambda K}$ and $e^{-\alpha D}$ (K and D are the kinetic operator and the double occupancy operator, respectively). The Gutzwiller-Jastrow wave function with the doublon-holon correlation operators are also employed. We have investigated the ground-state phase diagram of the two-dimensional Hubbard model[2, 3] and the two-dimensional three-band (d-p) model[4].

We carried out parallel computations in Monte Carlo calculations. In order to reduce statistical errors, we performed ~ 500 parallel calculations. Parallel computing is very essential to reduce Monte Carlo statistical errors.

The many-body wave function is written in the form $\psi^{(1)} = \exp(-\lambda K)P_G\psi_0$, where K denotes the kinetic energy part (non-interacting part) of the Hamiltonian and $P_G = P_G(g)$ is the Gutzwiller operator to control the double occupancy with the variational parameter g. ψ_0 indicates a trial wave function which is usually taken as the Fermi sea, the BCS wave function or the state with some magnetic (or charge) orders. We can improve the wave function systematically by multiplying by operators P_G and $e^{-\lambda K}$ repeatedly. We can consider $\psi^{(2)} = \exp(-\lambda' K)P_G(g')\psi^{(1)}$ for different variational parameters λ' and g'. This wave function is a very good many-body wave function because the ground-state energy is lowered greatly and the ground-state energy is lower than those that are evaluated by any other wave functions. We also employ the Jastrow-type wave function which is written as $\psi_J = P_G P_Q P_J \psi_0$ where P_J indicates a nearest-neighbor number correlation operator and P_Q controls the nearest-neighbor doublon-holon correlation.

2 Charge-ordered state coexisting with superconductivity in the Hubbard model

We have carriedi out a variational Monte Carlo simulation to examine the ground state in the optimal region of the two-dimensional Hubbard model on a square lattice. We can show that striped states are stable near the 1/8-doping region when t'/t is negative and U/t is large[5]. The one-particle state ψ_0 for stripe states are given by the eigenstate of the following Hamiltonian

$$H_{tri} = -\sum_{ij\sigma} t_{ij} c^{\dagger}_{i\sigma} c_{j\sigma} + \sum_{i\sigma} (\rho_i - \mathrm{sgn}(\sigma) m_i) n_{i\sigma}, \tag{1}$$

with $\rho_i = \rho \cos(\mathbf{Q}_c \cdot (\mathbf{r}_i - \mathbf{r}_0))$ and $m_i = m \sin(\mathbf{Q}_s \cdot (\mathbf{r}_i - \mathbf{r}_0))$. Here ρ and $m \equiv \Delta_{AF}$ are variational parameters. Two incommensurate wave vectors $\mathbf{Q}_c$ and $\mathbf{Q}_s$ characterize the charge and spin configurations, respectively. We set $\mathbf{Q}_c = 2\mathbf{Q}_s$. $\mathbf{r}_0$ denotes the position of the domain boundary. The vertical stripe is represented by $\mathbf{Q}_s = (\pi \pm 2\pi\delta, \pi)$ where δ stands for the incommensurability which defined as the inverse of the antiferromagnetic order in the x-direction. The charge modulation period is given by $\mathbf{Q}_c$.

We consider the case $t' = 0$. In this case, when U is as large as $U = 18t$, the antiferromagnetic state does not become stable[2] and thus a charge-ordered state can be stable in stead of stripes. This charge-ordered state can be called the nematic state. An important question is whether the charge-ordered state coexists with superconductivity. In the real space representation, the superconducting (SC) order parameter is assigned for each bond connecting two lattice points i and $i+\hat{\mu}$ where $\hat{\mu}$ indicates the unit vector in the μ-th direction. For d-wave pairing, we take the SC order parameter as $\Delta_{i,i+\hat{x}} = \Delta_s$ and $\Delta_{i,i+\hat{y}} = -\Delta_s$, where Δ_s is a real constant showing te magnitude of the SC order parameter. We can generalize this in several ways. For example,

$$\begin{aligned} \Delta_{i,i+\hat{x}} &= \Delta_s(\beta + (1-\beta)|\cos(\varphi(\mathbf{r}_i) - \pi/4)|), \\ \Delta_{i,i+\hat{y}} &= -\Delta_s(\beta + (1-\beta)|\cos(\varphi(\mathbf{r}_i))|), \end{aligned} \tag{2}$$

where β is a real constant in the range of $0 \leq \beta \leq 1$ and $\varphi(\mathbf{r}_i) = \mathbf{Q}_c \cdot (\mathbf{r}_i - \mathbf{r}_0)$. Δ_{ij} indicates the pure d-wave symmetry for $\beta = 1$ and is called the oscillating d-wave symmetry for $\beta = 0$.

We found that the charge-ordered state and superconductivity indeed coexist with each other when the doping rate $x =$ is near $1/8$ where we set $\delta = 1/8$[6]. In Fig. 1, we show the ground-state energy as a function of the superconducting order parameter Δ_s where we put $m = \Delta_{AF} = 0$ and $\rho = 0.01$. The d-wave state with charge nematic order is most stable for $U/t = 18$, $t' = 0$ and $x = 0.109375$.

3 Summary

We examined the ground state of the two-dimensional Hubbard model by using the advanced optimized variational Monte Carlo method. In the strong coupling region where U is ias large as or greater than the band width, the inhomogeneous state is stabilized when the doping rate x is is near $x = 0.125$. For $t' = 0$, the charge-ordered state is realized without magnetic order. The charge-ordered state can coexist with superconductivity as shown in Fig. 1.

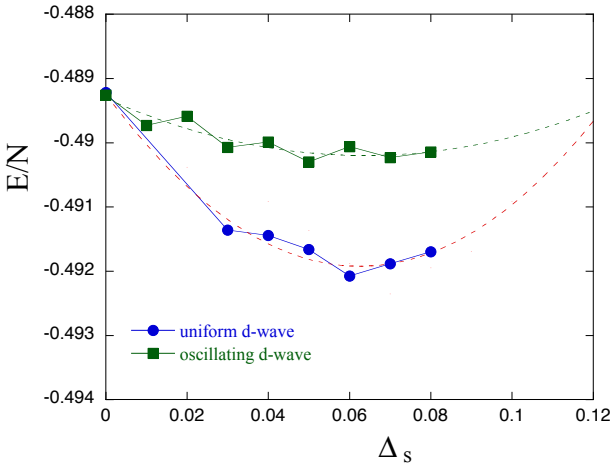

Figure 1: The ground-state energy as a function of the superconducting order parameter Δ_s for $N_e = 228$ (near 1/8-doping) on a 16×16 lattice, where we set $U = 18t$ and $t' = 0$. We employed the parameters given as $\Delta_{AF} = 0$, $\rho = 0.01$ and $\delta = 1/8$, We introduced the charge order parameter as $\rho = 0.01t$ for which the ground-state energy has a minimum. The circles show the energy for the uniform d-wave symmetry ($\beta = 1$) and the squares show that for the oscillating d-wave symmetry ($\beta = 0$).

References

[1] T. Yanagisawa et al., J. Phys. Soc. Jpn. 67, 3867 (1998).
T. Yanagisawa, Phys. Rev. B75, 224503 (2007) (arXiv: 0707.1929).

[2] T. Yanagisawa, J. Phys. Soc. Jpn. 85, 114707 (2016).
T. Yanagisawa, J. Phys. Soc. Jpn. 88, 054702 (2019).
T. Yanagisawa, Condensed Matter 4, 57 (2019).

[3] T. Yanagisawa, Phys. Lett. A403, 127382 (2021).

[4] T. Yanagisawa et al., EPL 134, 27004 (2021).

[5] M. Miyazaki, T. Yanagisawa, Phys. Lett. A448, 128276 (2022).

[6] T. Yanagisawa et al, preprint.

Many-body quantum simulations based on multi-scale space-time ansatz

Hiroshi SHINAOKA
Department of Physics, Saitama University, Saitama 338-8570

We have worked on the following topics in collaboration with co-workers.

(1) Parallelization quantics tensor train

We have implemented Julia libraries (TensorCrossInterpolation.jl, QuanticsGrids.jl) [1] for tensor cross interpolation and quantic tensor train [2,3]. A critical step toward practical calculations is parallelization of the algorithm. We have implemented a prototype parallelized code based on quantics tensor train in Julia. The code is still experimental and to be benchmarked on a HPC system.

(2) Hidden covalent insulator and spin excitations in SrRu2O6

We applied the density functional+dynamical mean-field theory to study the spin excitation spectra of SrRu2O6. We used DCore [4] and ALPS/CT-HYB [5]. After computing a self-consistent solution, we solved the Bethe-Salpeter equation to compute the dynamical susceptibility.

We found a good quantitative agreement with experimental spin excitation spectra. Depending on the size of the Hund's coupling J_H, the system chooses either the Mott insulator or covalent insulator state when magnetic ordering is not allowed. We found that the nature of the paramagnetic state has a negligible influence on the charge and spin excitation spectra.

(3) Comparative study of variational quantum circuits for quantum impurity models

We have developed compact ansatz for solving quantum impurity models using variational quantum circuits [7]. Our approaches are based on two ideas. First, we employed a compact physics-inspired ansatz, *k*-unitary cluster Jastrow ansatz, developed in the field of quantum chemistry. Second, we eliminated largely redundant variational parameters of physics-inspired ansatz associated with bath sites based on physical intuition. We benchmarked the new ansatzes and found that the compact anstazes outperform the original ansatz in terms of the number of variational parameters.

(4) Classical Monte Carlo simulation of J_1-J_2 *XY* Kagome antiferromagnet

We investigated the J_2-T phase diagram of the J_1-J_2 *XY* Kagome antiferromagnet using extensive classical Monte Carlo simulations based on non-local loop updates and replica-exchange Monte Carlo method [8]. Our code is implemented in Julia and use MPI parallelization. The obtained phase diagram

features Berezinskii-Kosterlitz-Thouless transitions of $q = 0$, $\sqrt{3} \times \sqrt{3}$ magnetic orders, and octupole orders, in addition to finite-temperature phase transitions of both ferrochiral and antiferrochiral long-range orders. We found a nontrivial first-order transition for antiferromagnetic $J_2/J_1 < 0$.

References

[1] https://tensor4all.org/

[2] H. Shinaoka, M. Wallerberger, Y. Murakami, K. Nogaki, R. Sakurai, P. Werner, and A. Kauch Phys. Rev. X **13**, 021015 (2023).

[3] M. K. Ritter, Y. N. Fernández, M. Wallerberger, J. von Delft, H. Shinaoka, and X. Waintal, Phys. Rev. Lett. **132**, 056501 (2024).

[4] H. Shinaoka, J. Otsuki, M. Kawamura, N. Takemori, K. Yoshimi, SciPost Phys. **10**, 117 (2021).

[5] H. Shinaoka, E. Gull, P. Werner, Comput. Phys. Commun. **215**, 128 (2017).

[6] D. Csontosová, H. Shinaoka, A. Hariki, and J. Kuneš, PRB **108**, 195137 (2023).

[7] R. Sakurai, O. J. Backhouse, G. H. Booth, W. Mizukami, and H. Shinaoka, Phys. Rev. Res. **6**, 023110 (2024).

[8] F. Kakizawa, T. Misawa, H. Shinaoka, PRB **109**, 014439 (2024).

Nonequilibrium dynamics in quantum systems driven by optical electric fields

Atsushi ONO
Department of Physics, Tohoku University, Sendai 980-8578

Research on controlling quantum systems through light irradiation has been actively pursued. We have conducted numerical simulations of the real-time dynamics of quantum systems driven by optical electric fields and explored the possibility of new classes of photoinduced phase transitions and ultrafast phenomena [1, 2], focusing on magnetic materials.

Among various magnetic structures, spin textures such as magnetic skyrmions have attracted interest owing to their intriguing transport and optical responses due to emergent fields. These noncoplanar magnetic structures are characterized by spin scalar chirality and are known to be stabilized by antisymmetric interactions such as the Dzyaloshinskii–Moriya interaction in systems with broken spatial inversion symmetry. However, limited studies have been conducted on the optical control of spin textures in centrosymmetric systems.

In a paper [1], we conducted numerical analyses of the real-time dynamics induced by terahertz electric fields in a ferromagnetic Kondo lattice model on a triangular lattice with spatial inversion symmetry. We numerically solved coupled equations of the von Neumann equation for electrons and the Landau–Lifshitz–Gilbert equation for localized spins. We found that, when a linearly polarized electric field is applied to the ground state of the ferromagnetic metallic phase, the ferromagnetic order melts within a time scale of approximately several hundred femtoseconds, followed by the emergence of a scalar chiral state after several picoseconds. Furthermore, it was revealed that the handedness of circular polarization controls the sign of chirality in this nonequilibrium scalar chiral state, as shown in Fig. 1. This photoinduced magnetic order is stabilized by the nonequilibrium distribution of electrons driven by the electric field and does not require antisymmetric interactions. This suggests that centrosymmetric itinerant magnets could be a promising platform for the ultrafast optical control of spin textures.

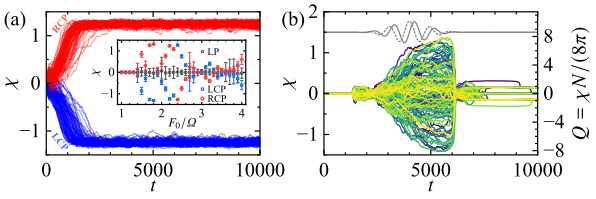

Figure 1: Temporal profiles of scalar chirality under (a) a circularly polarized continuous wave and (b) a linearly polarized pulse, for different spin configurations in the initial states, adapted from Ref. [1]. The inset in (a) shows the time-averaged chirality in the steady states as a function of the optical amplitude.

References

[1] A. Ono and Y. Akagi: Phys. Rev. B **108**, L100407 (2023).

[2] S. Imai and A. Ono: Phys. Rev. B **109**, L041303 (2024).

Theoretical study of BCS-BEC crossover in solid-state materials

Hiroshi WATANABE
Research Organization of Science and Technology, Ritsumeikan University
1-1-1 Noji-Higashi, Kusatsu-shi, Shiga 525-8577

In fermion systems with attractive interactions, the pairing mechanism of superconductivity (SC) or superfluidity is described by the Bardeen-Cooper-Schrieffer (BCS) theory in a weak interaction regime, while it is described by the Bose-Einstein condensation (BEC) in a strong interaction regime. They are smoothly connected in the intermediate regime, which is called BCS-BEC crossover. Recently, the possibility of BCS-BEC crossover in real materials has been reported in 2D gated semiconductor Li_xZrNCl, iron-based superconductor $FeSe_{1-x}S_x$, and 2D molecular superconductor κ-$(ET)_4Hg_{2.89}Br_8$. In strongly-correlated electron systems, it is much more difficult to identify the BCS-BEC crossover than in simple Fermi gas systems because of the unconventional (non-s-wave) gap symmetry and competition with various magnetic and/or charge orderings. To clarify the nature of BCS-BEC crossover in strongly-correlated electron systems, we study the extended Hubbard model for the κ-ET system [1, 2], which shows SC, several magnetic and/or charge orderings, and also the spin-liquid phase depending on the variety of anion layers. The hopping integral t_{ij}, on-site Coulomb interaction U, and the intersite Coulomb interaction V_{ij} are estimated from first-principles calculation. The ground state properties are analyzed with a variational Monte Carlo method. The system size for the calculation is N=24×24=576 unit cells (and thus 576×2=1152 molecules in total) and the computation has been done mainly with the system B at the ISSP Supercomputer Center.

In the non-doped case, the system undergoes a first-order transition from SC to Mott insulator with increasing U/t_{b1}, where t_{b1} denotes the largest hopping integral. This transition can be seen from the abrupt vanishing of the superconducting correlation function $P_{\rm SC}$. On the other hand, for the 5.5% hole-doped case, $P_{\rm SC}$ shows dome-shaped behavior with respect to U/t_{b1}, suggesting the BCS-BEC crossover (Fig. 1). Since the Mott insulator disappears with hole doping, SC survives in a large U/t_{b1} region at which the crossover realizes. These behaviors are consistent with the measured $T_{\rm c}$ and it suggests the occurrence of the BCS-BEC crossover in the κ-ET system.

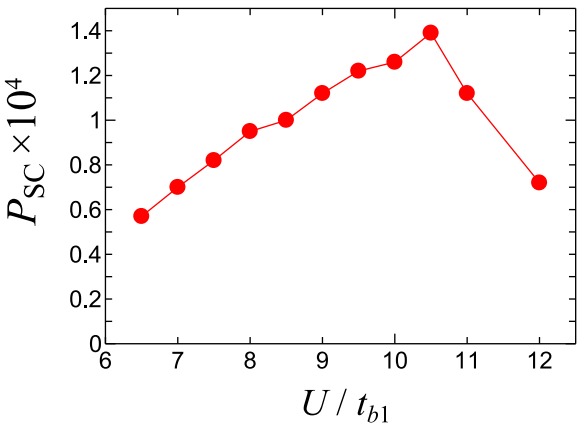

Figure 1: U/t_{b1} dependence of the superconducting correlation function $P_{\rm SC}$ of the extended Hubbard model with 5.5% hole doping.

References

[1] H. Watanabe, H. Seo, and S. Yunoki, J. Phys. Soc. Jpn. **86**, 033703 (2017).

[2] H. Watanabe, H. Seo, and S. Yunoki, Nat. Commun. **10**, 3167 (2019).

Compensated Ferrimagnetism with Colossal Spin Splitting in Organic compound $(EDO\text{-}TTF\text{-}I)_2ClO_4$

Akito Kobayashi[a], Taiki Kawamura[a], Kazuyoshi Yoshimi[b], Kenichiro Hashimoto[c], and Takahiro Misawa[b]

[a] *Department of Physics, Nagoya University, Nagoya 464-8602*

[b] *Institute for Solid State Physics, University of Tokyo, Kashiwa, Chiba 277-8581, Japan*

[c] *Department of Advanced Materials Science, University of Tokyo, Kashiwa, Chiba 277-8561, Japan*

Conventionally, it has been thought that collinear antiferromagnets, in which the spins are aligned antiparallel, do not exhibit unusual transport phenomena such as the generation of spin currents. However, recent theoretical research has revealed the existence of mysterious antiferromagnets, such as altermagnets and compensated ferrimagnets, which exhibit unique transport phenomena such as the anomalous Hall effect and spin current generation[1, 2, 3]. However, research on compensated ferrimagnetic materials has been limited to inorganic compounds such as alloys, and there have not been many examples of their implementation.

In this research, we discovered a simple method to realize compensated ferrimagnetism by using organic compounds with dimer structure. Specifically, we showed a simple design guideline that a compensated ferrimagnetic material can be realized if an antiferromagnetic order occurs in an organic compound in which two different dimers exist (Fig. 1). Furthermore, we also pointed out the possibility that compensated ferrimagnetism could be realized in the recently synthesized organic compound $(EDO\text{-}TTF\text{-}I)_2ClO_4$ using this mechanism. It was known that in this material, originally equivalent dimers become non-equivalent at low temperatures due to anion ordering. Using a strongly correlated first-principles calculation method, we analyzed the ordered phase that can theoretically be realized at low temperatures. As a result, we showed that the ground state is a compensated ferrimagnet[4]. This discovery sheds new light on the study of compensated ferrimagnets and shows that organic compounds provide an ideal stage for realizing compensated ferrimagnets.

References

[1] M. Naka et al., Nat. Commun. **10**, 1, (2019)

[2] H. van Leuken et al., Phys. Rev. Lett. **74**, 1171 (1995)

[3] S. Semboshi et al., Sci. Rep. **12**, 10687 (2022)

[4] T. Kawamura et al., Phys. Rev. Lett. **132**, 156502 (2024)

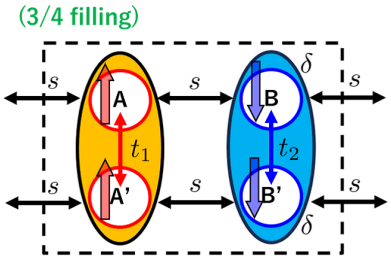

Figure 1: A non-equivalent dimer model that produces the compensated ferrimagnetism

Emergent inductance arising from a ferromagnetic domain wall under AC current

Kyohei Kado and Fumitaka Kagawa

Department of Physics,

Tokyo Institute of Technology, Tokyo 152-8551

The so-called "emergent inductor" describes a functionality that arises from the spin Berry phase associated with the interplay between flowing conduction electrons and an underlying magnetic texture [1]. Under the application of an AC electric current, the magnetic texture deforms in an AC manner as a result of a spin-transfer-torque (STT) effect. The flowing conduction electrons thus perceive a time-dependent U(1) gauge field, giving rise to an oscillating emergent electric field (EEF), which is described by:

$$e_i(r,t) = \frac{\hbar}{2|e|}\boldsymbol{m}(\boldsymbol{r},t) \cdot [\partial_i \boldsymbol{m}(\boldsymbol{r},t) \times \partial_t \boldsymbol{m}(\boldsymbol{r},t)], \quad (1)$$

where e (>0) is the elementary charge, $\boldsymbol{m}(\boldsymbol{r},t)$ is the unit vector of the local magnetic moment at position r and time t, and ∂_i (i = x, y, z) and ∂_t denote the spatial and time derivatives, respectively. As described in Eq. (1), changes in the magnetic texture in space and time are both essential for the emergence of an EEF. Even if the applied current density is weak and the magnetic texture is in the so-called pinned regime, the magnetic texture can elastically deform as a result of the STT effect by the current, I. Thus, under an AC current, $\partial_t \boldsymbol{m}(\boldsymbol{r},t)$ is finite in proportion to dI/dt, and an EEF may appear in an AC manner. Remarkably, it has been theoretically revealed that the AC-current-induced pinned dynamics of a helical magnetic texture1 give rise to an EEF with inductive characteristics (i.e., positive reactance) as a linear response to the applied AC current. Such a material showing the inductive response of the EEF is denoted an emergent inductor. Later, the close relationship between the emergent inductive reactance and the current-induced increase in magnetic-texture energy was also revealed. This new principle for inductive responses has drawn immediate attention from an application perspective because the inductance was inversely proportional to the sample cross-section size and therefore was presumed to be advantageous in terms of miniaturization over existing solenoid inductors.

In this study, we numerically investigated the emergent inductance due to a ferromagnetic domain wall under the application of an AC current. By referring to Landau-Lifshitz-Gilbert equation, we tracked the time evolution of the

spin texture under the current and calculated the emergent electric field from Eq. (1). The frequency dependence of the emergent inductance is shown in Fig. 1, in which L_1 and L_2 denote the real and imaginary parts of the emergent inductance, respectively.

We found that the Debye-like relaxation behaviour is obtained for the case of the intrinsic pinning (Fig. 1), whereas a resonance type is obtained for the case of the extrinsic pinning (not shown). The value of emergent inductance arising from single DW is on the order of 1 fH. Given that the detection limit in the inductance measurements is on the order of 1-10 nH, the required number of the domain walls is estimated to be 10^3-10^4.

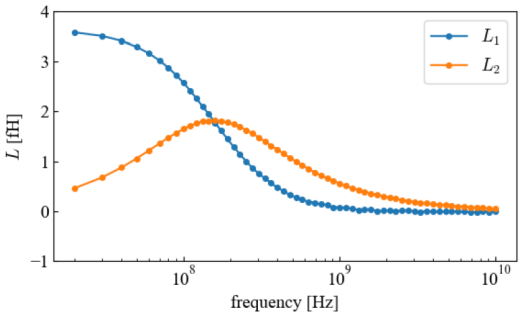

Fig. 1: Frequency dependence of the emergent inductance.

We used kugui and conducted micromagnetic simulation using MuMax3 respectively.

References

[1] N. Nagaosa, Jpn. J. Appl. Phys. **58**, 120909 (2019).

Theoretical study of thermoelectric properties in Heusler compounds using weak-coupling approaches

Kazutaka NISHIGUCHI
Graduate School of System Informatics, Kobe University
Rokkodai-Cho, Nada-Ku, Kobe 657-8501

Ferromagnetic fluctuations in Heusler alloy Fe_2VAl

Heusler compound Fe_2VAl is one of promising thermoelectric materials, which exhibits large power factor $P = \sigma S^2$ with σ and S being the electrical conductivity and Seebeck coefficient, respectively. On the other hand, the thermal the dimensionless figure of merit $ZT = \sigma S^2 T/\kappa$ is not so large yet reflecting its large thermal conductivity κ. Recently, it is experimentally observed in doped Fe_2VAl (i.e., $Fe_2V_{0.9}Cr_{0.1}Al_{0.9}Si_{0.1}$ and $Fe_{2.2}V_{0.8}Al_{1-y}Si_y$) as a weekly ferromagnetic material that ferromagnetic fluctuations enhance the thermoelectric properties such as S and P around the Curie temperature ($T_c = 285$ K). [1] It is not only a desirable property for practical use in realistic (room) temperatures, but also a fundamental and intriguing quantum phenomena where quantum fluctuations and thermoelectric effects are entangled by electron correlations.

Motivated above, we have studied electronic properties of Fe_2VAl using first-principles calculations based on the density functional theory (DFT) within the generalized gradient approximation (GGA). We performed DFT calculations with the Perdew–Burke–Ernzerhof (PBE) exchange-correlation functional for solids (PBEsol) and the projector augmented wave (PAW) method using The Vienna Ab Initio Simulation Package (VASP) [2] and Quantum ESPRESSO package (QE). [3]

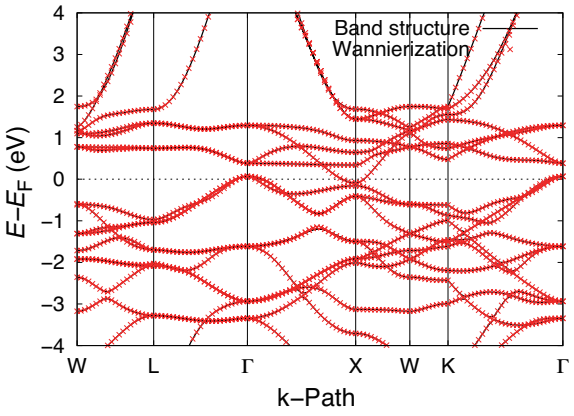

Figure 1: DFT band structure and Wannierization of Fe_2VAl.

Using the maximally localized Wannier functions, we could construct a low-energy effective model from the first- principles bands around the Fermi level. The effective model is composed of the Fe-3d, V-3d, and Al-2sp3 Wannier orbitals, namely, 19 orbitals. The DFT and structure and Wannier orbitals are shown in Fig. 1.

Furthermore, the obtained 19-orbital effective model was investigated using the random phase approximation (RPA). Figure 2 shows the total spin and charge susceptibility along the k-point path. It is clear that the spin fluctuations are dominant compared to the charge ones. Also, the obtained spin susceptibility has a peak at $q = (0, 0, 0)$, which reflects the ferromagnetic instability. This is consistent with the fact that Fe_2VAl exhibits the weak ferromagnetism.

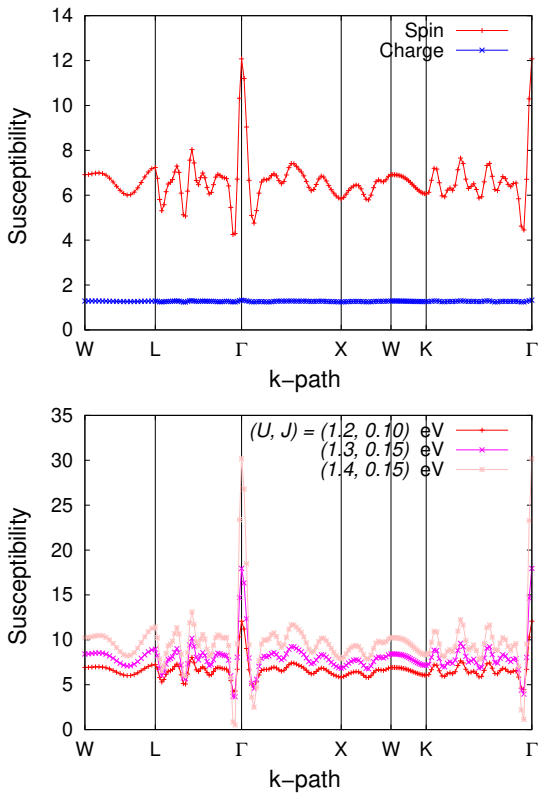

Figure 2: (Top) Total spin and charge susceptibility. (Bottom) Interaction dependence of the spin susceptibility. These are displayed along the k-point path.

Calculation conditions

We have performed the DFT calculations using the hybrid (MPI+OpenMP) parallel computing, where the parallelization over bands and k-points is used by VASP version 6.4.2 and QE version 7.2.

References

[1] N. Tsujii, A. Nishide, J. Hayakawa, and T. Mori: Sci. Adv. **5**, eaat5935 (2019).

[2] G. Kresse *et. al.*: Phys. Rev. B **47**, 558 (1993); Phys. Rev. B **49**, 14251 (1994); Computational Materials Science **6** (1996) 15–50; Phys. Rev. B **54**, 11169 (1996).

[3] P. Giannozzi *et. al.*: J. Phys.: Condens. Matter **21**, 395502 (2009) ; J. Phys.: Condens. Matter **29**, 465901 (2017) ; J. Chem. Phys. **152**, 154105 (2020).

[4] I. Souza, N. Marzari, and D. Vanderbilt: Phys. Rev. B **65**, 035109 (2001) ; A. A. Mostofi *et. al.*: Comput. Phys. Commun. **178** (2008) 685–699; A. A. Mostofi *et. al.*: Comput. Phys. Commun. **185** (2014) 2309–2310; G. Pizzi *et. al.*: J. Phys.: Condens. Matter **32**, 165902 (2020).

Calculating the Electronic Structure of Oxyhalides: Insights into their Optical Transitions

Takayuki MAKINO

University of Fukui, Bunkyo, Fukui, Fukui 910-8557

Bismuth oxychloride (BiOCl) is an oxyhalide compound with potential photocatalytic and optoelectronic applications. However, creating a flat surface has been challenging due to its low symmetry. Sun *et al.* successfully grew epitaxial layers of BiOCl with a flat surface and high crystallinity using a mist chemical vapor deposition method. This potentially facilitates the detailed characterization of their optical properties. [1,2]

Oxyhalides are classified as indirect-type semiconductors with an energy gap of approximately 2.9 eV. The optical response at the band-edge region of indirect semiconductors is considered weak, especially in the case of thin films. A recent report suggested that the formation of heterostructures between oxyhalides could turn an indirect-type into a direct-type semiconductor. This opens up possibilities for observing strong optical transitions even at the indirect-band-edge region. However, the grade suitable for detailed optical characterization having an atomically flat surface is only available in the form of thin films. This has discouraged researchers from studying the spectroscopic study of the indirect-type semiconductors at the band-edge region.

We conducted the optical characterization of BiOCl thin film on STO substrate by using a photoreflectance spectroscopy. We published a full paper [3] reporting the results of the optical characterization. In that article, it was necessary to display the energy-band structure for the clarification of the involved optical transition. That is why we calculated it despite several precedented theoretical works. The next paragraph is devoted to the description of the calculation procedure.

To calculate the band structures of BiOCl, we used the plane wave basis set PWscf package of Quantum ESPRESSO, an ab-initio density functional theory program with the plane wave basis, and a pseudopotential method. In addition to calculating band dispersion, QE can also perform structural optimization calculations, eigenfrequencies, and dielectric constants. First-principles calculations within the framework of density functional theory (DFT) is performed to analyze the structural and electronic properties of BiOCl. In this calculation, we neglected the contribution from $SrTiO_3$. For the atomic coordinates of BiOCl, the structure that has been adopted in the previous DFT calculations,

consistent with the experimental results, was adopted. To find the influence of the electron density on the exchange correlation energies of ions, we have used the LDA functional, which belongs to the class of Methfessel-Paxton functionals. The Brillouin zone (BZ) was integrated using an 8×8×8 centered Monkhorst-Pack k-point grid. As a precaution, it is necessary to adopt a value for which the cutoff energy converges. Our cutoff energy is $10^{(-8)}$ Ry. The Bi, Cl, and O atoms are represented by norm-conserving pseudopotentials, and the kinetic energy and charge density cutoffs are chosen to be 50 and 400 Ry, respectively. Methfessel-Paxton smearing of the Fermi-Dirac distribution, with a smearing width of 0.02 Ry.

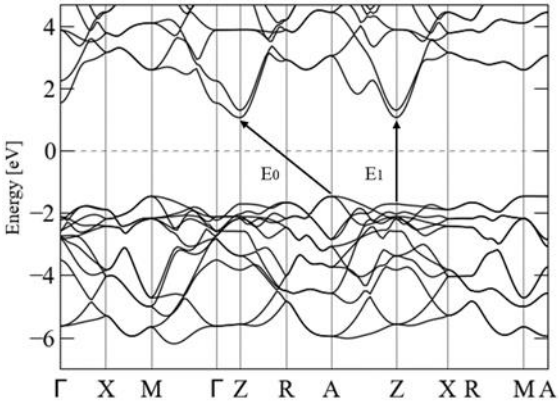

Fig. 1: Electronic structure of BiOCl.

References

[1] K. T. Drisya, S. Cortés-Lagunes, A.-L. Garduño-Jiménez, R. N. Mohan, N. Pineda-Aguilar, A. C. Mera, R. Zanella, and J. C. Durán-Álvarez, J. Environ. Chem. Eng. **10**, 108495 (2022).

[2] Z. Sun, D. Oka, and T. Fukumura, Chem. Commun. **56**, 9481 (2020).

[3] T. Nishiwaki, T. Makino, Z. Sun, D. Oka, T. Fukumura: Jpn. J. Appl. Phys, **63**, 02SP09 (2024).

Band Engineering and Electron Correlation Effects in Artificially Stacked Systems

Toshikaze KARIYADO

Research Center for Materials Nanoarchitectonics,

National Institute for Materials Science, Tsukuba, Ibaraki 305-0044

It is known that a zigzag edge of graphene hosts a flat edge band dispersion that leads to edge magnetization due to the large density of states [1,2]. On the other hand, it is also known that a proper edge decoration to a zigzag edge removes the flat band and the edge magnetization [3,4]. From these, we expect that partial completion of the edge decoration can be used to control magnetism at the graphene edge, for instance, to have a localized spin-1/2 state at the edge.

To demonstrate this idea, we investigated electronic and magnetic properties of some graphene nanoflakes with partially completed decorations at the edge (Inset of Fig. 1). We have done structural relaxations and band calculations based on the density functional theory using Quantum Espresso and OpenMX packages. Since the investigated flakes have large number of atoms, we need large computational resources. Both packages are nicely parallelized for large scale calculations, and OpenMX package is designed to handle large number of atoms. Note that the hydrogenation at the edge is applied terminated by hydrogen in actual calculations for stability.

Figure 1 shows a typical (Kohn-Sham) energies obtained in the spin density functional theory calculation. The result indicates that there appears a localized spin-1/2 state at the upper middle part of the flake in the inset of Fig. 1. It is an interesting future work to extend the same idea to variety of flake structures, to see spin-spin interaction when there are multiple localized states.

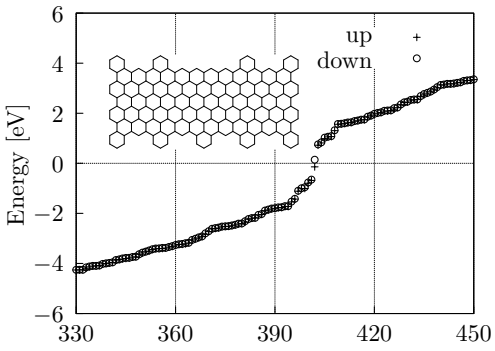

Fig. 1: Spin resolved energy spectrum.

References

[1] M. Fujita *et al.*, J. Phys. Soc. Jpn. **65**, 1920 (1996).

[2] G. Z. Madga *et al.*, Nature **514**, 608 (2014).

[3] D. J. Klein and L. Bytautas, J. Phys. Chem. A **103**, 5196 (1999).

[4] A. Narita et al., Nature Chem. **6**, 126 (2014).